Relay Selection Protocols for Relay-Assisted Free-Space Optical Systems

Nestor D. Chatzidiamantis, Diomidis S. Michalopoulos, Emmanouil E. Kriezis, George K. Karagiannidis, and Robert Schober

***Abstract*—We investigate transmission protocols for relay-assisted free-space optical (FSO) systems, when multiple parallel relays are employed and there is no direct link between the source and the destination. As alternatives to all-active FSO relaying, where all the available relays transmit concurrently, we propose schemes that select only a single relay to participate in the communication between the source and the destination in each transmission slot. The selection is based on the channel state information obtained either from all or from the last used FSO links. Thus, the need for synchronization of the relays' transmissions is avoided, while the slowly varying nature of the atmospheric channel is exploited. For the considered relay selection and all-active relaying schemes, novel closed-form expressions for the outage performance are derived, assuming the versatile Gamma–Gamma channel model. In addition, based on the derived analytical results, the problem of optimizing the optical power resources of the FSO links is addressed. Optimal and more computationally attractive suboptimal solutions are proposed that lead to a power efficient system design. Numerical results for equal and non-equal length FSO links illustrate the merits of the proposed relay selection protocols compared to the all-active scheme and demonstrate the significant power savings offered by the proposed power allocation schemes.**

***Index Terms*—Cooperative diversity; Distributed switch and stay relaying; Free-space optical communications; Power allocation; Relay-assisted communications; Relay selection.**

I. Introduction

The constant need for higher data rates in support of high-speed applications has led to the development of the free-space optical (FSO) communication technology. Operating at unlicensed optical frequencies, FSO systems offer the potential of broadband capacity at low cost [1], and, therefore, they present an attractive remedy for the "last-mile" problem. However, despite their major advantages, the widespread deployment of FSO systems is hampered by several major impairments, which have their origin in the propagation of optical signals through the atmosphere [2].

Manuscript received August 13, 2012; revised October 9, 2012; accepted November 14, 2012; published December 21, 2012 (Doc. ID 174258).

Nestor D. Chatzidiamantis (e-mail: nestoras@auth.gr), Emmanouil E. Kriezis, and George K. Karagiannidis are with the Department of Electrical and Computer Engineering, Aristotle University of Thessaloniki, GR-54124 Thessaloniki, Greece.

Diomidis S. Michalopoulos and Robert Schober are with the Department of Electrical and Computer Engineering, The University of British Columbia, Vancouver, BC V6T 1Z4, Canada.

Digital Object Identifier 10.1364/JOCN.5.000092

In the past, several techniques have been applied in FSO systems to mitigate the degrading effects of the atmospheric channel, including error control coding in conjunction with interleaving [3], multiple-symbol detection [4], and spatial diversity [5–7]. Among these techniques, spatial diversity, which is realized by deploying multiple transmit and/or receive apertures, is particularly attractive, since it offers significant performance gains by introducing additional degrees of freedom in the spatial dimension. Thus, numerous FSO systems with multiple co-located transmit and/or receive apertures, referred to as multiple-input multiple-output (MIMO) FSO systems, have been proposed in the technical literature [5–7]. However, in practice, MIMO FSO systems may not always be able to offer the gains promised by theory. This happens in cases where the assumption that all the links of the MIMO FSO system are affected by independent channel fading becomes invalid [7]. Furthermore, since both the path loss and the fading statistics of the channel are distance dependent, a large number of transmit and/or receive apertures is required in long-range links in order to achieve the desired performance gains, thus increasing the complexity of MIMO FSO systems.

In order to overcome such limitations, relay-assisted communication has recently been introduced in FSO systems as an alternative approach to achieve spatial diversity [8–11]. The main idea lies in the fact that, by employing multiple relay nodes with line-of-sight (LOS) to both the source and the destination, a virtual multiple-aperture system is created, often referred to as a cooperative diversity system. An advantage of this virtual multiple-aperture system, as opposed to MIMO FSO systems, is that multiple paths are spatially separated from each other, thus ensuring independence of the corresponding fading channels. In [8], various relaying configurations (cooperative diversity and multihop) were investigated under the assumption of a log-normal channel model. Subsequently, several coding schemes for three-way cooperative diversity FSO systems with a single relay and a direct link between the source and the destination were proposed in [9], while the performance of such systems was investigated in [10,11] assuming amplify-and-forward and decode-and-forward (DF) relaying strategies, respectively. It is emphasized that in all these works, all the available relays participated in the communication between the source and the destination, a technique that requires perfect synchronization between the relays, since the FSO signals must arrive simultaneously at the destination. In practice, however, and particularly in the case of dissimilar FSO links between the source and the relays (or between the relays and the destination), synchronization of the transmissions of multiple

1943-0620/13/010092-12/$15.00 © 2013 Optical Society of America

relays is a cumbersome task, especially for the signaling rates of interest and large numbers of relays.

In view of the above, in this paper we present alternative transmission protocols, which avoid the concurrent activation of multiple relays and can be applied to relay-assisted FSO systems with no LOS between the source and the destination. Under the assumption that, for the signaling rates of interest, the atmospheric channel does not vary within one frame, the channel state information (CSI) can be easily obtained for all or some of the links involved. On this basis, the presented protocols activate only a single relay in each transmission slot, thus avoiding the need for synchronization between the relays. It should be noted that the concept of selecting a single relay has also been introduced for quantum-limited FSO cooperative systems in [12]. Unlike [12], in our analysis we include the effect of background noise, which significantly degrades the reception of FSO signals [5,6]. The contributions of this paper can be summarized as follows:

- Two different types of relay selection protocol for cooperative FSO systems are proposed. Specifically, we present the select-max protocol, which selects the relay that maximizes an appropriately defined metric and requires CSI from all the available FSO links, and the distributed switch and stay (DSS) protocol, which switches between two relays and requires CSI only from the FSO links used in the previous transmission slot.
- Assuming the versatile Gamma–Gamma channel model [2], background noise limited reception, and DF relay nodes, we derive novel closed-form analytical expressions for the outage performance of the proposed transmission schemes. As a benchmark, we also investigate the outage performance of the scheme where all the available relays transmit simultaneously, thus extending the analysis presented in [8] to the case of the Gamma–Gamma channel model.
- Based on the outage analysis, we address the problem of optimizing the allocation of the optical power resources to the FSO links for minimization of the outage probability. Optimal as well as more computationally attractive suboptimal power allocation rules are proposed, which take into account the distance-dependent nature of atmospheric effects, and increase the overall power efficiency of the relay-assisted FSO system under consideration.

II. The System Model

The system model under consideration is depicted in Fig. 1. In particular, we consider an intensity modulation direct detection (IM/DD) FSO system without LOS between the source, S, and the destination, D, and the communication between these two terminals is achieved with the aid of N relays, denoted by R_i, $i \in \{1,\ldots,N\}$. The source node is equipped with a multiple-aperture transmitter, with each of the apertures pointing in the direction of the corresponding relay. Additionally, the source employs an optical switch,[1] which, depending on the mode of operation, either allows simultaneous transmission from all the transmit apertures or selects the direction of transmission by switching between the transmit apertures. At the destination node, all optical signals transmitted by each relay are collected by the receiving detector and simultaneously detected. For the system model under consideration, the following assumptions are made:

1) Statistical independence among the S–R_i and R_i–D FSO links is assumed. This can be achieved by placing the multiple transmit apertures just a few centimeters apart [6] and the relaying terminals in different directions. Hence, the atmospheric effects that influence the optical beams received by D via the multiple available paths can be considered uncorrelated.
2) All optical transmitters are equipped with optical amplifiers that adjust the optical power transmitted in each link. Furthermore, all the receivers are background noise limited, which means that the background noise becomes dominant compared to other noise components (such as thermal, signal dependent, and dark noise).
3) The relaying terminals use a threshold-based DF protocol. That is, they fully decode the received signal and retransmit it to the destination only if the signal-to-noise ratio (SNR) of the received FSO signal exceeds a given decoding threshold.
4) Binary pulse position modulation[2] (BPPM) is employed.

A. The Signal and Channel Model

For an FSO link connecting two terminals A and B, the received optical signal at the photodetector of B is given by

$$\mathbf{r}_B = \begin{bmatrix} r^s \\ r^n \end{bmatrix} = \begin{bmatrix} \mathscr{R}T_b\left(\rho_{AB}P_t h_{AB} + P_b\right) + n^s \\ \mathscr{R}T_b P_b + n^n \end{bmatrix}, \tag{1}$$

where r^s and r^n represent the signal and non-signal slots of the BPPM symbol, respectively, while $\rho_{AB}P_t$ and P_b denote the average optical signal power transmitted from A and the background radiation power incident on the photodetector of B, respectively. Furthermore, ρ_{AB} represents the percentage of the total optical power P_t allocated to the FSO link between terminals A and B, h_{AB} is the term that models the channel effects of the link, $\mathscr{R}$ is the photodetector's responsivity, T_b is the time duration of both the signal and non-signal slots of the BPPM symbol, and n^s and n^n are the additive noise samples in the signal and non-signal slots, respectively. Since background noise limited reception is assumed at the receiver, each noise term can be modeled as additive white Gaussian noise, with zero mean and variance σ_n^2 [5,6].

Due to atmospheric effects, the channel gain of the FSO link under consideration can be modeled as

$$h_{AB} = \bar{h}_{AB}\tilde{h}_{AB}, \tag{2}$$

where $\bar{h}_{AB}$ accounts for the path loss due to weather effects and geometric spread loss, and $\tilde{h}_{AB}$ represents irradiance

[1] Optical switches can be implemented with either spatial light modulators (SLMs) [13, Ch. (27)] or optical micro-electromechanical systems (MEMSs) [14]. Furthermore, taking into consideration the coherence time of the atmospheric channel, the switching times of such optical switches can follow the variations of the atmospheric channel.

[2] We note that the relaying protocols that are described in the analysis that follows are independent of the type of modulation and depend only on the received SNR of each link.

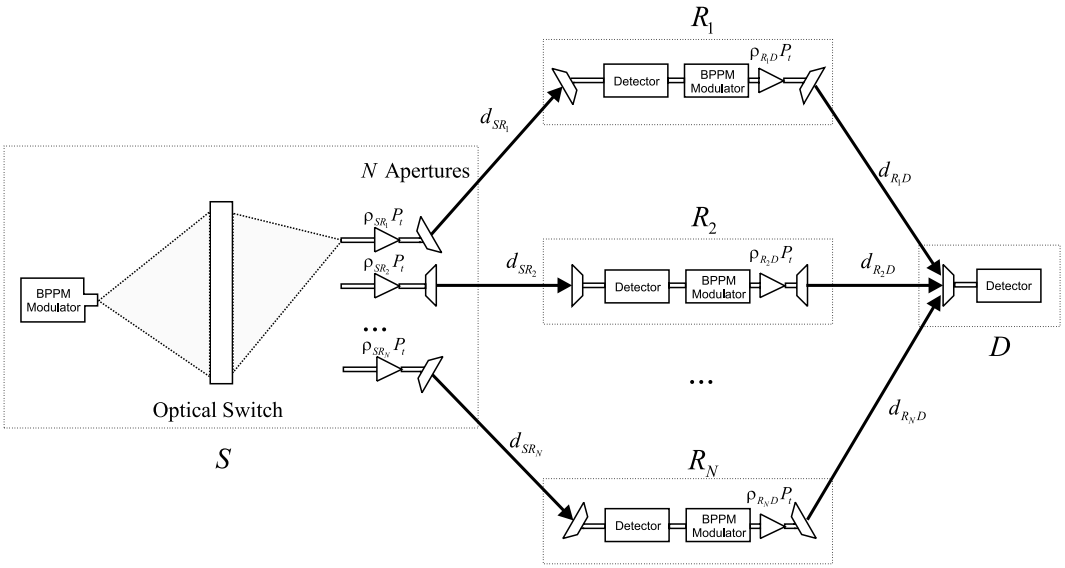

Fig. 1. Block diagram of the relay-assisted FSO system under consideration.

fluctuations caused by atmospheric turbulence. Both $\bar{h}_{AB}$ and $\tilde{h}_{AB}$ are time-variant, yet at very different time scales. The path loss coefficient varies on the order of hours, while the turbulence-induced fading varies on the order of 1–100 ms [6]. Thus, taking into consideration the signaling rates of interest, which range from hundreds to thousands of Mbps, the channel gain h_{AB} can be considered as constant over a given transmission slot, which consists of hundreds of thousands (or even millions) of symbols, and varies in an uncorrelated fashion in each slot.

The path loss coefficient can be calculated by combining the Beer–Lambert law [2] with the geometric loss formula [1, pp. 44], yielding

$$\bar{h}_{AB} = \frac{D_R^2}{\left(D_T + \theta_T d_{AB}\right)^2} \exp\left(-v d_{AB}\right), \tag{3}$$

where D_R and D_T are the receiver and transmitter aperture diameters, respectively; θ_T is the optical beam's divergence angle (in mrad), d_{AB} is the link distance (in km) between nodes A and B, and v is the weather-dependent attenuation coefficient (in 1/km).

Under a wide range of atmospheric conditions, turbulence-induced fading can be statistically characterized by the well-known Gamma–Gamma distribution [2]. The probability density function (pdf) for this model is given by

$$f_{\tilde{h}_{AB}}(x) = \frac{2\left(\alpha_{AB}\beta_{AB}\right)^{\frac{\alpha_{AB}+\beta_{AB}}{2}}}{\Gamma(\alpha_{AB})\Gamma(\beta_{AB})} x^{\frac{\alpha_{AB}+\beta_{AB}}{2}-1} \times K_{\alpha_{AB}-\beta_{AB}}\left(2\sqrt{\alpha_{AB}\beta_{AB}x}\right), \tag{4}$$

where $\Gamma(\cdot)$ is the Gamma function [15, Eq. (8.310)] and $K_v(\cdot)$ is the vth order modified Bessel function of the second kind [15, Eq. (8.432/9)], while its cumulative density function (cdf) is given by [16, Eq. (7)]

$$F_{\tilde{h}_{AB}}(x) = \frac{1}{\Gamma\left(\alpha_{AB}\right)\Gamma\left(\beta_{AB}\right)} \times G_{1,3}^{2,1}\left[\alpha_{AB}\beta_{AB}x \middle| \begin{matrix} 1 \\ \alpha_{AB}, \beta_{AB}, 0 \end{matrix}\right], \tag{5}$$

where $G_{p,q}^{m,n}[\cdot]$ is Meijer's G-function [15, Eq. (9.301)]. Furthermore, α_{AB} and β_{AB} are parameters related to the effective atmospheric conditions of the link, calculated assuming plane wave propagation and ignoring aperture averaging effects [2, Eqs. (9.41), (9.46), (9.138)]. They also depend on the Rytov variance defined by $\sigma_R^2 = 1.23 C_n^2 \left(\frac{2\pi}{\lambda}\right)^{\frac{7}{6}} d_{AB}^{\frac{11}{6}}$, where d_{AB} is the link distance, C_n^2 denotes the weather-dependent index of the refraction structure parameter, and λ is the wavelength of the optical carrier. It should be noted that the presented system model can be readily extended to include aperture averaging effects and other wave propagation models by modifying the calculation of the α_{AB} and β_{AB} parameters accordingly [2].

After removing the constant bias $\mathscr{R}T_bP_b$ from both PPM slots, the instantaneous SNR of the link can be defined as [8]

$$\gamma_{AB} = \bar{\gamma}_{AB}\tilde{h}_{AB}^2, \tag{6}$$

where $\bar{\gamma}_{AB}$ denotes the average SNR of the link, given by

$$\bar{\gamma}_{AB} = \frac{\mathscr{R}^2 \rho_{AB}^2 T_b^2 P_t^2 \bar{h}_{AB}^2}{2\sigma_n^2}. \tag{7}$$

B. The Mode of Operation

Throughout this work, three different cooperative relaying protocols are considered: the all-active protocol, where all the

available relays are activated, the select-max protocol, and the DSS protocol, both of which are based on the concept of selecting a single relay. It should be noted that the all-active protocol was originally presented in [8] and its performance will be used as a benchmark in the comparison with the proposed relay selection protocols.

1) All-Active: In this relaying scheme, the source activates all relays and the total power is divided between all the available FSO links. Since the relay nodes operate in the DF mode, only the relays that successfully decode the received optical signal remodulate the intensity of the optical carrier and forward the information to the destination. At the destination, all the received optical signals are added. Hence, assuming perfect synchronization, the output of the combiner can be expressed as

$$\mathbf{r}_D = \begin{bmatrix} \mathscr{R} T_b \left(\sum_{m \in \mathbf{D}} \rho_{R_m D} h_{R_m D} P_t + P_b \right) + n^s \\ \mathscr{R} T_b P_b + n^n \end{bmatrix}, \tag{8}$$

where $\mathbf{D}$ denotes the decoding set formed by the relays that have successfully decoded the signal. Since the total power is divided between all available links, it follows that $\sum_{i=1}^{N} (\rho_{SR_i} + \rho_{R_i D}) = 1$.

The advantage of this scheme is that CSI is not required either at the transmitter or at the receiver side, since the source transmits to all the relays, regardless of their channel gain. However, since it is assumed that all the signals arrive at the destination at the same time, this scheme requires accurate timing synchronization in order to account for the different propagation delays of the different paths, thus resulting in high complexity.

2) Select-Max: This relaying protocol selects a single relay out of the set of N available relays in each transmission slot. In particular, the relay that maximizes an appropriately defined metric is selected. This metric accounts for both the S–R_i and R_i–D links and reflects the quality of the ith end-to-end path. Here, we adopt the minimum value of the intermediate link SNRs,

$$\gamma_i = \min(\gamma_{SR_i}, \gamma_{R_i D}), \tag{9}$$

as the quality measure of the ith end-to-end path, which will be referred to as the "*min-equivalent SNR*" throughout the paper. Note that Eq. (9) represents an outage-based definition of the selection metric, in the sense that an outage on the ith end-to-end link occurs if γ_i falls below the outage threshold SNR. Hence, the single relay that is activated in the select-max relaying protocol, R_b, is selected according to the rule

$$b = \underset{i \in \{1,\ldots,N\}}{\operatorname{argmax}} \gamma_i. \tag{10}$$

Since a single relay is activated in the select-max protocol, the total available optical power is divided between the S–R_b and R_b–D links, i.e., $\rho_{SR_b} + \rho_{R_b D} = 1$, and in the case that R_b has successfully decoded the received optical signal, i.e., $b \in \mathbf{D}$, the signal at the destination can be expressed as

$$\mathbf{r}_D = \begin{bmatrix} \mathscr{R} T_b \left(\rho_{R_b D} P_t h_{R_b D} + P_b \right) + n^s \\ \mathscr{R} T_b P_b + n^n \end{bmatrix}. \tag{11}$$

This relaying scheme requires the CSI of all the available S–R_i and R_i–D FSO links in order to perform the selection process. The CSI can be estimated by some signaling process that takes advantage of the slowly varying nature of the FSO channel.[3] Here, each receiver estimates the corresponding link CSI and feeds it back to the source through a reliable low-rate RF feedback link. It is emphasized that since only one end-to-end path is activated in each transmission slot, only one signal arrives at the destination and, thus, synchronization between the relays is not needed.

3) Distributed Switch and Stay: Assuming that there are two relays available, the DSS protocol selects one of them to take part in the communication between the source and the destination in a switch and stay fashion [17]. More specifically, in each transmission slot the destination compares the min-equivalent SNR of the active end-to-end path with a switching threshold, denoted by T. If this SNR is smaller than T, the destination notifies the source and the other available relay is selected for taking part in the communication, regardless of its end-to-end performance metric.

Mathematically speaking, denoting the two available relays by R_1 and R_2 and the min-equivalent SNR of the ith end-to-end path during the jth transmission period by γ_i^j, the active relay in the jth transmission period, R_b^j, is determined as follows:

$$\text{if } R_b^{j-1} = R_1, \text{ then } R_b^j = \begin{cases} R_1 \text{ when } \gamma_1^j \geq T \\ R_2 \text{ when } \gamma_1^j < T \end{cases}, \tag{12}$$

and

$$\text{if } R_b^{j-1} = R_2, \text{ then } R_b^j = \begin{cases} R_2 \text{ when } \gamma_2^j \geq T \\ R_1 \text{ when } \gamma_2^j < T. \end{cases} \tag{13}$$

Hence, in the case that R_b^j has successfully decoded the received signal, the optical signal at the destination is given by

$$\mathbf{r}_D = \begin{bmatrix} \mathscr{R} T_b \left(\rho_{R_b^j D} P_t h_{R_b^j D} + P_b \right) + n^s \\ \mathscr{R} T_b P_b + n^n \end{bmatrix}. \tag{14}$$

Since in this protocol only a single relay assists in the communication between the source and the destination, the power allocation rule of the select-max protocol also holds for DSS relaying.

When there are more than two available relays in the system, i.e., $N > 2$, a modified version of the DSS protocol

[3] For example, pilot symbols may be inserted in each transmission slot. Taking into consideration that each transmission slot comprises hundreds of thousands of consecutive symbols, the insertion of a few pilot symbols (e.g., less than 10) will not cause a significant overhead.

initially sorts all the available paths based on their *"max-equivalent"* distance, defined as

$$d_i = \max\left(d_{SR_i}, d_{R_iD}\right), \tag{15}$$

with $i = 1,\ldots,N$, and then uses the two relays that correspond to the paths with the minimum max-equivalent distances as R_1 and R_2. It should be noted that the max-equivalent distance is indicative of the path's end-to-end performance, taking into consideration that both the path loss and the Rytov variance are monotonically increasing with respect to the link distance.

The simplicity of the DSS protocol compared to the select-max protocol lies in the fact that only the CSI of the active end-to-end path is required for the selection process, resulting in a lower implementation complexity. Furthermore, as in the select-max scheme, no synchronization among the relays is needed, since only one end-to-end path is activated in each transmission slot.

III. Outage Probability Analysis

At a given data transmission rate, r_0, the outage probability is defined as

$$\mathscr{P}_o = \Pr\left\{C(\gamma) < r_0\right\}, \tag{16}$$

where $C(\cdot)$ is the instantaneous capacity, which is defined in [18, Eq. (23)] and is a function of the instantaneous SNR. Since $C(\cdot)$ is monotonically increasing with respect to γ, Eq. (16) can be equivalently rewritten as

$$\mathscr{P}_o = \Pr\left\{\gamma < \gamma_{th}\right\}, \tag{17}$$

where $\gamma_{th} = C^{-1}(r_0)$ denotes the threshold SNR. If the SNR, γ, drops below γ_{th}, an outage occurs, implying that the signal cannot be decoded with arbitrarily low error probability at the receiver. Henceforth, it is assumed that the threshold SNR, γ_{th}, is identical for all participating links.

A. The Outage Probability of the Intermediate Links

Since DF relaying is considered, an outage event in any of the intermediate links may lead to an outage of the overall relaying scheme. Therefore, the calculation of the outage probability of each intermediate link is considered as a building block for the outage probability of the relaying schemes under investigation.

By combining Eq. (6) with Eq. (17), the outage probability of the FSO link between nodes A and B is obtained as

$$\mathscr{P}_{o,AB} = \Pr\left\{\frac{\mathscr{R}^2 T_b^2 \rho_{AB}^2 P_t^2 h_{AB}^2}{2\sigma_n^2} < \gamma_{th}\right\}, \tag{18}$$

which can be equivalently rewritten as

$$\mathscr{P}_{o,AB} = \Pr\left\{\tilde{h}_{AB} < \frac{1}{\bar{h}_{AB}\rho_{AB}P_M}\right\}, \tag{19}$$

where P_M is the power margin given by $P_M = \frac{\mathscr{R}T_b P_t}{\sigma_n\sqrt{2\gamma_{th}}}$. Using Eq. (5), the outage probability of the FSO link between nodes A and B can be analytically evaluated for any α_{AB} and β_{AB} as

$$\mathscr{P}_{o,AB} = F_{\tilde{h}_{AB}}\left(\frac{1}{\bar{h}_{AB}\rho_{AB}P_M}\right). \tag{20}$$

To gain more physical insight from Eq. (20), it is meaningful to explore the outage probability in the high power margin regime.

Theorem 1. For high values of the power margin, the outage probability of the FSO link between nodes A and B can be approximated as

$$\mathscr{P}_{o,AB} \approx \frac{\Gamma\left(p_{AB} - q_{AB}\right)}{\Gamma(\alpha_{AB})\Gamma(\beta_{AB})} \frac{\left(\frac{\alpha_{AB}\beta_{AB}}{\bar{h}_{AB}P_M\rho_{AB}}\right)^{q_{AB}}}{q_{AB}}, \quad (\alpha_{AB} - \beta_{AB}) \notin \mathbb{Z}, \tag{21}$$

where $p_{AB} = \max(\alpha_{AB}, \beta_{AB})$ and $q_{AB} = \min(\alpha_{AB}, \beta_{AB})$.

Proof. A proof is provided in Appendix A. □

It should be noted that in the analysis that follows it is assumed that $(\alpha_{AB} - \beta_{AB}) \notin \mathbb{Z}$ holds for every possible FSO link. Although this condition may seem restrictive, it is realistic in practical applications.

B. The Outage Probability of All-Active Relaying

In this scheme, an outage occurs when either the decoding set $\mathbf{D}$ is empty or the SNR of the multiple-input single-output link between the decoding relays and the destination falls below the outage threshold. Hence, the outage probability of this scheme can be expressed as [8, Eq. (30)]

$$\mathscr{P}_{o,\text{all-act}} = \sum_{n=1}^{2^N} \Pr\left\{\sum_{m\in\mathscr{S}(n)} \rho_{R_mD} h_{R_mD} < \frac{1}{P_M}\right\} \times \Pr\{\mathscr{S}(n)\}, \tag{22}$$

where $\mathscr{S}(n)$ denotes the nth possible decoding set, 2^N is the total number of decoding sets, and $\Pr\{\mathscr{S}(n)\}$ is the probability of event $\{\mathbf{D} = \mathscr{S}(n)\}$ given by

$$\Pr\{\mathscr{S}(n)\} = \prod_{m\in\mathscr{S}(n)} \left(1 - \mathscr{P}_{o,SR_m}\right) \prod_{m\notin\mathscr{S}(n)} \mathscr{P}_{o,SR_m}. \tag{23}$$

In order to evaluate Eq. (22), the cdf of the sum of weighted non-identical Gamma–Gamma variates, $h_{\mathscr{S}(n)} = \sum_{m\in\mathscr{S}(n)} \rho_{R_mD} h_{R_mD}$, needs to be derived first. However, to the best of the authors' knowledge, there are no closed-form analytical expressions for the exact distribution of the sum of non-identical Gamma–Gamma variates. Therefore, the numerical method of [19, Eq. (9.186)] can be applied to evaluate the cdf of $h_{\mathscr{S}(n)}$, denoted as $F_{h_{\mathscr{S}(n)}}(\cdot)$, using the moment generating function (MGF) of the channel gain of the R_m–D FSO link, which is given by [20, Eq. (4)]. Hence, by combining Eq. (22) with Eq. (20), the outage probability of the

all-active relaying protocol in Gamma–Gamma fading can be written as

$$\mathscr{P}_{o,\text{all-act}} = \sum_{n=1}^{2^N} \prod_{m\in\mathscr{S}(n)} \left(1 - F_{\tilde{h}_{SR_m}}\left(\frac{1}{\bar{h}_{SR_m}\rho_{SR_m}P_M}\right)\right) \times F_{h_{\mathscr{S}(n)}}\left(\frac{1}{P_M}\right) \prod_{m\notin\mathscr{S}(n)} F_{\tilde{h}_{SR_m}}\left(\frac{1}{\bar{h}_{SR_m}\rho_{SR_m}P_M}\right). \quad (24)$$

Asymptotic Analysis: In order to gain more physical insight into the performance of the relaying protocol under consideration, we further consider the high power margin regime, i.e., when $P_M \to \infty$. In order to perform this analysis, an asymptotic expression for $F_{h_{\mathscr{S}(n)}}(\cdot)$ needs to be derived first.

Lemma 1. For high values of the power margin, the cdf of $h_{\mathscr{S}(n)}$ can be approximated as

$$F_{h_{\mathscr{S}(n)}}(x) \approx \frac{\prod_{m\in\mathscr{S}(n)}\left(\frac{\alpha_{R_mD}\beta_{R_mD}}{\bar{h}_{R_mD}\rho_{R_mD}}\right)^{q_{R_mD}}}{\left(\sum_{m\in\mathscr{S}(n)} q_{R_mD}\right)\Gamma\left(\sum_{m\in\mathscr{S}(n)} q_{R_mD}\right)} \times \prod_{m\in\mathscr{S}(n)}\left(\frac{\Gamma\left(q_{R_mD}\right)\Gamma\left(p_{R_mD}-q_{R_mD}\right)}{\Gamma\left(\alpha_{R_mD}\right)\Gamma\left(\beta_{R_mD}\right)}\right) \times x^{\left(\sum_{m\in\mathscr{S}(n)} q_{R_mD}\right)}. \quad (25)$$

Proof. A proof is provided in Appendix B. □

The asymptotic expression for the outage probability of the all-active relaying scheme is obtained by first observing that in the high power margin regime, i.e., $P_M \to \infty$, Eq. (23) can be approximated by

$$\Pr\{\mathscr{S}(n)\} \approx \prod_{m\notin\mathscr{S}(n)} \mathscr{P}_{o,SR_m}. \quad (26)$$

Hence, by combining Eq. (22) with Eqs. (21), (25) and (26), the asymptotic expression in Eq. (27) (given in Box 1) is obtained.

C. The Outage Probability of Select-Max Relaying

In the select-max protocol a single relay out of the N available relays is selected according to the selection rule in Eq. (10). Hence, the outage probability of the relaying scheme under consideration is given by

$$\mathscr{P}_{o,\text{sel-max}} = \mathscr{P}_o\{R_1 \cap \cdots \cap R_N\} = \prod_{b=1}^{N} \mathscr{P}_{o,R_b}, \quad (28)$$

where $\mathscr{P}_{o,R_b}$ denotes the probability of outage when only relay R_b is active. Given that R_b is active, an outage occurs when either R_b or D has not decoded the information successfully, i.e.,

$$\mathscr{P}_{o,R_b} = \Pr\{(\gamma_{SR_b} < \gamma_{th}) \cup (\gamma_{R_bD} < \gamma_{th})\} = 1 - (1 - \mathscr{P}_{o,SR_b})(1 - \mathscr{P}_{o,R_bD}). \quad (29)$$

By combining Eq. (28) with Eqs. (29) and (20), an accurate analytical expression for the performance evaluation of the select-max relaying scheme in Gamma–Gamma turbulence-induced fading can be derived as

$$\mathscr{P}_{o,\text{sel-max}} = \prod_{b=1}^{N}\left(1 - \left(1 - F_{\tilde{h}_{SR_b}}\left(\frac{1}{\bar{h}_{SR_b}\rho_{SR_b}P_M}\right)\right) \times \left(1 - F_{\tilde{h}_{R_bD}}\left(\frac{1}{\bar{h}_{R_bD}\rho_{R_bD}P_M}\right)\right)\right). \quad (30)$$

Asymptotic Analysis: In order to gain more physical insight into the performance of the relaying protocol under consideration, we investigate its asymptotic behavior when $P_M \to \infty$ in the ensuing theorem.

Theorem 2. For high values of the power margin, the outage probability of the select-max relaying scheme can be approximated by

$$\mathscr{P}_{o,\text{sel-max}} \approx \prod_{b=1}^{N}\left(\frac{\Gamma\left(p_{SR_b}-q_{SR_b}\right)}{q_{SR_b}\Gamma\left(\alpha_{SR_b}\right)\Gamma\left(\beta_{SR_b}\right)}\left(\frac{\alpha_{SR_b}\beta_{SR_b}}{\bar{h}_{SR_b}\rho_{SR_b}P_M}\right)^{q_{SR_b}} + \frac{\Gamma\left(p_{R_bD}-q_{R_bD}\right)}{q_{R_bD}\Gamma\left(\alpha_{R_bD}\right)\Gamma\left(\beta_{R_bD}\right)}\left(\frac{\alpha_{R_bD}\beta_{R_bD}}{\bar{h}_{R_bD}\rho_{R_bD}P_M}\right)^{q_{R_bD}}\right). \quad (31)$$

Proof. The proof starts by observing that as $P_M \to \infty$ the probability of outage given that relay R_b is active can be approximated by

$$\mathscr{P}_{o,R_b} \approx \mathscr{P}_{o,SR_b} + \mathscr{P}_{o,R_bD}. \quad (32)$$

Hence, by combining Eq. (28) with Eqs. (21) and (32), the asymptotic expression in Eq. (31) is obtained. This concludes the proof. □

D. The Outage Probability of DSS Relaying

In the DSS protocol, the selection of the single relay that takes part in the communication is based on Eqs. (12) and (13). Hence, an outage occurs when there is an outage either in the end-to-end link of the first relay, given that the first relay is selected in the jth transmission slot, or in the end-to-end link of the second relay, given that the second relay is selected in the jth transmission. Mathematically speaking, the outage probability of DSS is expressed as

$$\mathscr{P}_{o,DSS} = \Pr\left\{\left(R_b^j = R_1\right) \cap \left(\gamma_1^j < \gamma_{th}\right)\right\} + \Pr\left\{\left(R_b^j = R_2\right) \cap \left(\gamma_2^j < \gamma_{th}\right)\right\}. \quad (33)$$

The following theorem provides an accurate analytical expression for the performance of the DSS relaying scheme.

$$\mathscr{P}_{o,\text{all-act}} \approx \sum_{n=1}^{2^N} \prod_{m\notin\mathscr{S}(n)} \left(\frac{\pi\Gamma\left(p_{SR_m}-q_{SR_m}\right)}{\Gamma\left(\alpha_{SR_m}\right)\Gamma\left(\beta_{SR_m}\right)} \frac{\left(\frac{\alpha_{SR_m}\beta_{SR_m}}{\bar{h}_{SR_m}\rho_{SR_m}}\right)^{q_{SR_m}}}{q_{SR_m}} \right) \times \frac{\prod_{m\in\mathscr{S}(n)} \left(\frac{\alpha_{R_mD}\beta_{R_mD}}{\bar{h}_{R_mD}\rho_{R_mD}}\right)^{q_{R_mD}} \frac{\Gamma(q_{R_mD})\Gamma(p_{R_mD}-q_{R_mD})}{\Gamma(\alpha_{R_mD})\Gamma(\beta_{R_mD})}}{\left(\sum_{m\in\mathscr{S}(n)} q_{R_mD}\right)\Gamma\left(\sum_{m\in\mathscr{S}(n)} q_{R_mD}\right)} \left(\frac{1}{P_M}\right)^{\left(\sum_{m\notin\mathscr{S}(n)} q_{SR_m}+\sum_{m\in\mathscr{S}(n)} q_{R_mD}\right)} \tag{27}$$

Box 1.

Theorem 3. The probability of outage of a relay-assisted FSO system that employs the DSS relaying protocol is given by

$$\mathscr{P}_{o,DSS} = \begin{cases} \dfrac{F_{h_1}\left(\frac{1}{\bar{T}}\right)F_{h_2}\left(\frac{1}{\bar{T}}\right)\left(F_{h_1}\left(\frac{1}{P_M}\right)+F_{h_2}\left(\frac{1}{P_M}\right)\right)}{F_{h_1}\left(\frac{1}{\bar{T}}\right)+F_{h_2}\left(\frac{1}{\bar{T}}\right)}, & \bar{T}\le P_M, \\ \dfrac{F_{h_1}\left(\frac{1}{\bar{T}}\right)F_{h_2}\left(\frac{1}{\bar{T}}\right)\left(F_{h_1}\left(\frac{1}{P_M}\right)+F_{h_2}\left(\frac{1}{P_M}\right)-2\right)}{F_{h_1}\left(\frac{1}{\bar{T}}\right)+F_{h_2}\left(\frac{1}{\bar{T}}\right)} \\ +\dfrac{F_{h_1}\left(\frac{1}{P_M}\right)F_{h_2}\left(\frac{1}{\bar{T}}\right)+F_{h_1}\left(\frac{1}{\bar{T}}\right)F_{h_2}\left(\frac{1}{P_M}\right)}{F_{h_1}\left(\frac{1}{\bar{T}}\right)+F_{h_2}\left(\frac{1}{\bar{T}}\right)}, & \bar{T}>P_M, \end{cases} \tag{34}$$

where

$$F_{h_i}(x) = 1-\left(1-F_{\bar{h}_{SR_i}}\left(\frac{1}{\bar{h}_{SR_i}\rho_{SR_i}x}\right)\right) \times \left(1-F_{\bar{h}_{R_iD}}\left(\frac{1}{\bar{h}_{R_iD}\rho_{R_iD}x}\right)\right), \tag{35}$$

and $\bar{T}=\frac{\mathscr{R}T_bP_t}{\sqrt{2T}\sigma_n}$.

Proof. The proof starts by following the analysis of [19, Section (9.9.1.2)] and rewriting Eq. (33) as

$$\mathscr{P}_{o,DSS} = \begin{cases} \dfrac{F_{\gamma_1}(T)F_{\gamma_2}(T)\left(F_{\gamma_1}(\gamma_{th})+F_{\gamma_2}(\gamma_{th})\right)}{F_{\gamma_1}(T)+F_{\gamma_2}(T)}, & \gamma_{th}\le T, \\ \dfrac{F_{\gamma_1}(T)F_{\gamma_2}(T)\left(\Pr\{\gamma_1<\gamma_{th}\}+F_{\gamma_2}(\gamma_{th})-2\right)}{F_{\gamma_1}(T)+F_{\gamma_2}(T)} \\ +\dfrac{\left(F_{\gamma_1}(\gamma_{th})F_{\gamma_2}(T)+F_{\gamma_1}(T)F_{\gamma_2}(\gamma_{th})\right)}{F_{\gamma_1}(T)+F_{\gamma_2}(T)}, & \gamma_{th}>T, \end{cases} \tag{36}$$

where

$$F_{\gamma_i}(x)=\Pr\{\gamma_i<x\}. \tag{37}$$

According to [21, pp. 141], we have

$$F_{\gamma_i}(x) = 1-\left(1-\Pr\{\gamma_{SR_i}<x\}\right) \times \left(1-\Pr\{\gamma_{SR_i}<x\}\right), \tag{38}$$

which can be reduced to Eq. (35). Hence, by combining Eq. (35) with Eq. (36), Eq. (34) is obtained. This concludes the proof. □

Corollary 1. The performance of the DSS relaying scheme is maximized when $\bar{T}=P_M$ and in that case it becomes equal to that of the select-max scheme with two relays, R_1 and R_2.

Proof. Following the analysis in [19, (Ch. 9.9.1.1)], the performance of DSS relaying is maximized for $\bar{T}=P_M$. In that case, Eq. (34) yields

$$\mathscr{P}_{o,DSS}=\prod_{i=1}^{2}\left(1-\left(1-\mathscr{P}_{o,SR_i}\right)\left(1-\mathscr{P}_{o,R_iD}\right)\right). \tag{39}$$

Equation (39) is equivalent to Eq. (30), when only relays R_1 and R_2 are available to the system. This concludes the proof. □

IV. Optimal Power Allocation

In this section, we are interested in optimizing the optical power resources in both the S–R_i and R_i–D links, in order to minimize the outage probability of the relay-assisted FSO system for a given total optical power. This constraint on the total optical power aims at the design of power efficient relay-assisted FSO systems that take into account the distance dependent atmospheric effects. It also serves as a reference point for a fair comparison between the relaying protocols under consideration. In the following, we optimize the parameters ρ_{SR_i} and ρ_{R_iD} for each of the relaying protocols under consideration.

A. Power Allocation in the All-Active Protocol

Since in the all-active scheme the power is divided among all the underlying links, minimization of its outage probability is subject to two constraints: the total power budget of all links equals P_t and the maximum optical power emitted from each transmitter is not greater than $P_{\max}$, which is mandated by eye safety regulations [22]. Consequently, the optimum power allocation can be found by solving the following optimization problem:

$$\min \mathscr{P}_{o,\text{all-act}} \quad \text{subject to} \begin{cases} \sum_{m=1}^{N}\left(\rho_{SR_m}+\rho_{R_mD}\right)=1, \\ 0<\rho_{SR_m},\rho_{R_mD}\le\rho_o, \quad m=1,\ldots,N, \end{cases} \tag{40}$$

where $\mathscr{P}_{o,\text{all-act}}$ is given by Eq. (24) and $\rho_o=\frac{P_{\max}}{P_t}$ with $\frac{1}{2}\le\rho_o\le 1$. For the exact outage expression in Eq. (24), it is difficult to find the optimum solution for the problem in Eq. (40), even with numerical methods, due to the involvement of Meijer's G-functions. Therefore, the asymptotic expression of Eq. (27) is used as the objective function instead and

the optimization problem that arises is a geometric program that can be numerically solved using numerical optimization techniques, such as the interior point method [23, Section 14].

Since the computation of the exact solution is cumbersome, even if Eq. (27) is adopted as the objective function, the following suboptimal power allocation scheme for all-active relaying is proposed, which is based on maximizing $\bar{\gamma}_{SR_i}$ and $\bar{\gamma}_{R_iD}$ simultaneously (or equivalently minimizing $\frac{1}{\bar{\gamma}_{SR_i}}$ and $\frac{1}{\bar{\gamma}_{R_iD}}$), subject to the constraints in Eq. (40).

Proposition 1. For all-active relaying, the fraction of the total optical power which is allocated to each link is given by

$$\rho_{SR_i} = \frac{1}{\sum_{m=1}^{N}\left(\sqrt{\frac{\bar{h}_{SR_i}}{\bar{h}_{SR_m}}} + \sqrt{\frac{\bar{h}_{SR_i}}{\bar{h}_{R_mD}}}\right)} \tag{41}$$

and

$$\rho_{R_iD} = \frac{1}{\sum_{m=1}^{N}\left(\sqrt{\frac{\bar{h}_{R_iD}}{\bar{h}_{SR_m}}} + \sqrt{\frac{\bar{h}_{R_iD}}{\bar{h}_{R_mD}}}\right)} \tag{42}$$

for the S–R_i and R_i–D links, respectively, with $i = 1,\ldots,N$. In the case that some of the power allocation parameters calculated by Eqs. (41) and (42) exceed ρ_o, the above power allocation rule is reformulated as

$$\rho_{SR_i} = \rho_o \quad \text{and} \quad \rho_{R_iD} = \rho_o, \quad \text{if } SR_i, R_iD \in \mathbf{T}, \tag{43}$$

$$\rho_{SR_i} = \frac{1 - |\mathbf{T}|\rho_o}{\sum_{SR_m \notin \mathbf{T}} \sqrt{\frac{\bar{h}_{SR_i}}{\bar{h}_{SR_m}}} + \sum_{R_mD \notin \mathbf{T}} \sqrt{\frac{\bar{h}_{SR_i}}{\bar{h}_{R_mD}}}}, \quad \text{if } SR_i \notin \mathbf{T}, \tag{44}$$

and

$$\rho_{R_iD} = \frac{1 - |\mathbf{T}|\rho_o}{\sum_{SR_m \notin \mathbf{T}} \sqrt{\frac{\bar{h}_{R_iD}}{\bar{h}_{SR_m}}} + \sum_{R_mD \notin \mathbf{T}} \sqrt{\frac{\bar{h}_{R_iD}}{\bar{h}_{R_mD}}}}, \quad \text{if } R_iD \notin \mathbf{T}, \tag{45}$$

where $\mathbf{T}$ is the set formed by the FSO links whose power allocation parameters exceed ρ_o, and $|\cdot|$ represents the cardinality of a set.

B. Power Allocation in the Select-Max Protocol

Similarly to the all-active scheme, the outage probability of the select-max protocol can also be minimized by optimizing the optical power resources that are allocated to each of the links. However, in this scheme, both the objective function and the constraints are different from those in Eq. (40).

Since the total optical power is divided only between the S–R_b and R_b–D links of the active relay, the problem is formulated as

$$\text{subject to } \begin{cases} \min \mathscr{P}_{o,R_b} \\ \rho_{SR_b} + \rho_{R_bD} = 1, \\ 0 < \rho_{SR_b}, \quad \rho_{R_bD} \le \rho_o, \end{cases} \tag{46}$$

where $\mathscr{P}_{o,R_b}$ is the probability of outage when R_b is active given by Eq. (29). Due to the involvement of Meijer's G-functions, it is again difficult, if not impossible, to find the optimum solution if the exact expression in Eq. (29) is used as the objective function, even with numerical methods. Therefore, the asymptotic expression in Eq. (32) is employed and hence the power allocation optimization problem is reformulated as in Eq. (47). It should be noted that the optimization problem defined in Eq. (47) is convex, thus leading to a unique optimal solution.

$$\min \left(\frac{\Gamma\left(p_{SR_b} - q_{SR_b}\right)}{\Gamma\left(\alpha_{SR_b}\right)\Gamma\left(\beta_{SR_b}\right) q_{SR_b}} \left(\frac{\alpha_{SR_b}\beta_{SR_b}}{\bar{h}_{SR_b}} \right)^{q_{SR_b}} \right.$$
$$\left. + \frac{\Gamma\left(p_{R_bD} - q_{R_bD}\right)}{\Gamma\left(\alpha_{R_bD}\right)\Gamma\left(\beta_{R_bD}\right) q_{R_bD}} \left(\frac{\alpha_{R_bD}\beta_{R_bD}}{\bar{h}_{R_bD}} \right)^{q_{R_bD}} \right) \tag{47}$$
$$\text{subject to } \begin{cases} \rho_{SR_b} + \rho_{R_bD} = 1, \\ 0 < \rho_{SR_b}, \rho_{R_bD} \le \rho_o. \end{cases}$$

The following theorem specifies the power allocation parameters for the select-max protocol that minimize the probability of outage.

Theorem 4. The power allocation parameters that minimize the outage probability of an FSO system employing select-max relaying and operating in Gamma–Gamma turbulence-induced fading are given by

$$\rho_{SR_b} = \begin{cases} \zeta_{SR_b}, & \text{if } \zeta_{SR_b} < \rho_o \text{ and } \zeta_{R_bD} < \rho_o, \\ \rho_o, & \text{if } \zeta_{SR_b} \ge \rho_o, \\ 1 - \rho_o, & \text{if } \zeta_{R_bD} \ge \rho_o, \end{cases} \tag{48}$$

and

$$\rho_{R_bD} = \begin{cases} \zeta_{R_bD}, & \text{if } \zeta_{SR_b} < \rho_o \text{ and } \zeta_{R_bD} < \rho_o, \\ 1 - \rho_o, & \text{if } \zeta_{SR_b} \ge \rho_o, \\ \rho_o, & \text{if } \zeta_{R_bD} \ge \rho_o, \end{cases} \tag{49}$$

for the S–R_b and R_b–D links, respectively, where $b = 1,\ldots,N$, $\zeta_{SR_b} = (\delta_{SR_b} t_0)^{\frac{1}{q_{SR_b}+1}}$, $\zeta_{R_bD} = (\delta_{R_bD} t_0)^{\frac{1}{q_{R_bD}+1}}$, $\delta_{SR_b} = \frac{\Gamma(p_{SR_b} - q_{SR_b})}{\Gamma(\alpha_{SR_b})\Gamma(\beta_{SR_b})} \left(\frac{\alpha_{SR_b}\beta_{SR_b}}{\bar{h}_{SR_b} P_M} \right)^{q_{SR_b}}$, $\delta_{R_bD} = \frac{\Gamma(p_{R_bD} - q_{R_bD})}{\Gamma(\alpha_{R_bD})\Gamma(\beta_{R_bD})} \times \left(\frac{\alpha_{R_bD}\beta_{R_bD}}{\bar{h}_{R_bD} P_M} \right)^{q_{R_bD}}$, and $t_0 \in \left[0, \min\left(\frac{1}{\delta_{SR_b}}, \frac{1}{\delta_{R_bD}} \right)\right]$ is the unique real positive root of

$$\mathscr{S}(t) = \delta_{SR_b}^{\frac{1}{q_{SR_b}+1}} t^{\frac{1}{q_{SR_b}+1}} + \delta_{R_bD}^{\frac{1}{q_{R_bD}+1}} t^{\frac{1}{q_{R_bD}+1}} - 1. \tag{50}$$

Proof. The proof starts by first ignoring the inequality constraint in the optimization problem in Eq. (47) and defining the Lagrangian function as

$$\mathscr{J} = \frac{\delta_{SR_b}}{\rho_{SR_b}^{q_{SR_b}}} + \frac{\delta_{R_bD}}{\rho_{R_bD}^{q_{R_bD}}} - \Lambda\left(\rho_{SR_b} + \rho_{R_bD}\right), \tag{51}$$

where Λ is the Lagrange multiplier. After setting $\frac{\partial \mathscr{J}}{\partial \rho_{SR_b}} = 0$ and $\frac{\partial \mathscr{J}}{\partial \rho_{R_bD}} = 0$, and using the equality constraint $\rho_{SR_b} + \rho_{R_bD} = 1$, it is straightforward to show that the optimum power allocation coefficients ρ_{SR_b} and ρ_{R_bD} equal ζ_{SR_b} and ζ_{R_bD}, respectively, where $t_0 = -\frac{1}{\Lambda}$ is the root of $\mathscr{S}(t)$ taking values in the interval $\left[0, \min\left(\frac{1}{\delta_{SR_b}}, \frac{1}{\delta_{R_bD}}\right)\right]$. It should be noted that $\mathscr{S}(t)$ has a unique positive root that lies in this interval; this can be proved by applying the intermediate value theorem of continuous functions, which shows that $\mathscr{S}(t)$ has at least one real positive root in the interval $\left[0, \min\left(\frac{1}{\delta_{SR_b}}, \frac{1}{\delta_{R_bD}}\right)\right]$ in conjunction with Descartes' rule of signs [24], which shows that this root is unique. In the case that the value of any of the derived parameters ζ_{SR_b} and ζ_{R_bD} exceeds ρ_o, the solution is modified according to Eqs. (52) and (53) in order to satisfy the inequality constraint of Eq. (47). □

In order to avoid solving the polynomial $\mathscr{S}(t)$, the following suboptimal power allocation scheme for select-max relaying is proposed, which is based on minimizing simultaneously $\frac{1}{\bar{\gamma}_{SR_b}}$ and $\frac{1}{\bar{\gamma}_{R_bD}}$, subject to the constraints in Eq. (47).

Proposition 2. A suboptimal solution to the power allocation problem of the select-max relaying scheme is to set ρ_{SR_b} and ρ_{R_bD} as follows:

$$\rho_{SR_b} = \begin{cases} \kappa_{SR_b}, & \text{if } \kappa_{SR_b} < \rho_o \text{ and } \kappa_{R_bD} < \rho_o, \\ \rho_o, & \text{if } \kappa_{SR_b} \geq \rho_o, \\ 1-\rho_o, & \text{if } \kappa_{R_bD} \geq \rho_o, \end{cases} \tag{52}$$

and

$$\rho_{R_bD} = \begin{cases} \kappa_{R_bD}, & \text{if } \kappa_{SR_b} < \rho_o \text{ and } \kappa_{R_bD} < \rho_o, \\ \rho_o, & \text{if } \kappa_{R_bD} \geq \rho_o, \\ 1-\rho_o, & \text{if } \kappa_{SR_b} \geq \rho_o, \end{cases} \tag{53}$$

where $b = 1,\ldots,N$, $\kappa_{SR_b} = \frac{1}{\left(1+\sqrt{\frac{\bar{h}_{SR_b}}{\bar{h}_{R_bD}}}\right)}$, and $\kappa_{R_bD} = \frac{1}{\left(1+\sqrt{\frac{\bar{h}_{R_bD}}{\bar{h}_{SR_b}}}\right)}$.

C. Power Allocation in the DSS Protocol

Since a single relay is activated in each transmission slot for the DSS protocol, the optimal power allocation scheme is obtained by minimizing the outage probability of the active end-to-end path. Hence, the optimization problem that has to be solved in this case is identical to the problem in Eq. (47) and, therefore, the optimal and suboptimal power allocation schemes for the select-max protocol can also be employed for DSS relaying.

V. Numerical Results and Discussion

In this section, we illustrate numerical results for the outage performance of the considered relaying protocols, using the derived analytical expressions. In the following, we consider a relay-assisted FSO system with $\lambda = 1550$ nm and transmit and receive aperture diameters of $D_R = D_T = 20$ cm. Furthermore, we assume clear weather conditions with a visibility of 10 km, which corresponds to a weather-dependent attenuation coefficient of $v = 0.1\ \frac{1}{\text{km}}$ and an index of refraction structure parameter of $C_n^2 = 2 \times 10^{-14}\ \text{m}^{-\frac{2}{3}}$, while the maximum optical power that can be emitted from each laser is $P_{\max} = P_t = 40$ mW, i.e., $\rho_o = 1$.

Figure 2 depicts the outage performance of the presented relaying protocols for various numbers of relays, when the link distance is identical for all S–R_i and R_i–D links and the optical power is equally divided between the active relays. Specifically, analytical results for the outage probability of a relay-assisted FSO system with a link distance of 2 km are plotted, as functions of the power margin for $N = 2,3,4$ relays using the exact and asymptotic outage expressions for each of the considered relaying protocols. We assumed $\rho_{SR_i} = \rho_{R_iD} = \frac{1}{2N}$ for the all-active and $\rho_{SR_i} = \rho_{R_iD} = \frac{1}{2}$ for the select-max and DSS protocols, respectively. As benchmarks, Monte Carlo (MC) simulation results and the performance of an FSO system with $N = 1$, which is independent of the employed relaying protocol, are also shown in Fig. 2. As can be observed, there is an excellent match between the simulation and the analytical results for every value of N, verifying the presented theoretical analysis. Moreover, it is obvious that the select-max relaying scheme has a better performance compared to the all-active scheme in every case examined (performance gains of 2, 4, and 5 dB are observed for $N = 2$, 3, and 4, respectively). This result is intuitively pleasing, since the select-max protocol selects in each transmission slot the best end-to-end path out of the N available paths and allocates the total available optical power only to this path. Furthermore, when increasing the number of relays in the select-max and all-active protocols, it is observed that the outage performance is significantly improved with respect to the single relay FSO system. In contrast, although the DSS scheme with the optimum threshold offers significant performance improvement for $N = 2$ (its performance is identical to the select-max performance of $N = 2$), it remains unaffected by the increase of the number of relays.

Figure 3 depicts the outage performance of a relay-assisted FSO system employing the presented protocols and assuming different distances for each of the S–R_i and R_i–D FSO links. Specifically, two different system configurations are investigated. In the first system configuration, $N = 2$ and the link distances are given by vectors $d_{\text{SR}} = \{2, 1.5\}$ and $d_{\text{RD}} = \{1, 2.5\}$, with the elements of the vectors representing the distances (in km) of the S–R_i and R_i–D links, respectively, while in the second configuration $N = 3$ and the link distances are given by $d_{\text{SR}} = \{2, 1.5, 1\}$ and $d_{\text{RD}} = \{1, 2.5, 3\}$. Figure 3 reveals that the select-max relaying scheme offers significant performance gains compared to the all-active scheme, also for non-equal link distances. In particular, for the first configuration a gain of 2.5 dB compared to the all-active scheme is offered, while for the second configuration the offered gain is 3 dB. Furthermore, it can be easily observed that,

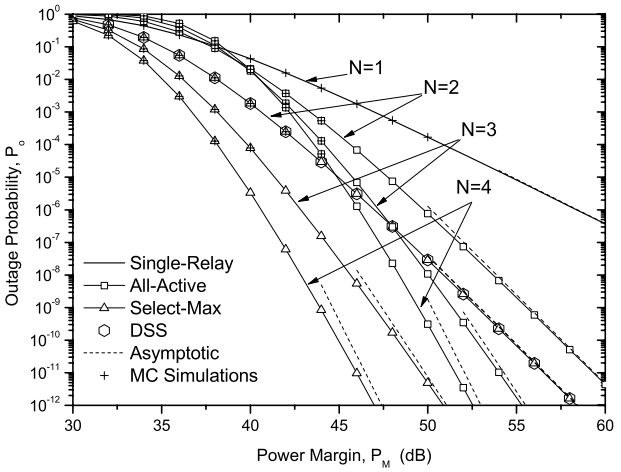

Fig. 2. Comparison of the relaying protocols for a relay-assisted FSO system with $d_{SR_i} = d_{R_iD} = 2$ km, $i \in \{1,\ldots,N\}$.

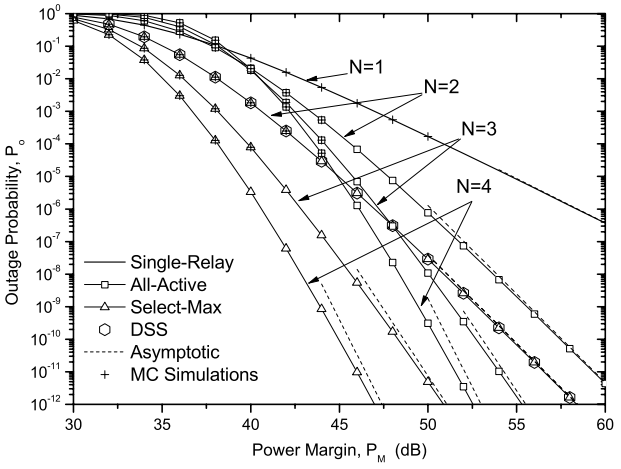

Fig. 3. Comparison of the relaying protocols for different relay-assisted FSO configurations: $N = 2$, $d_{\mathrm{SR}} = \{2, 1.5\}$, $d_{\mathrm{RD}} = \{1, 2.5\}$ (in km) and $N = 3$, $d_{\mathrm{SR}} = \{2, 1.5, 1\}$, $d_{\mathrm{RD}} = \{1, 2.5, 3\}$ (in km).

although in the second configuration the number of relays has been increased and the performances of both all-active and select-max relaying have been improved, DSS with optimized threshold remains unaffected by this increase and its performance remains identical with the performance for the first configuration. This was expected, since DSS uses only two end-to-end paths (those with the minimum max-equivalent distance) and, therefore, the addition of extra paths with larger max-equivalent distances will not improve the performance of this protocol. Finally, we note that the simulation and analytical results are again in excellent agreement.

Figure 4 illustrates the effect of power allocation in relay-assisted FSO systems employing the relaying protocols under consideration. Specifically, the performances of the optimal and proposed suboptimal power allocation schemes are presented along with equal power allocation, when the second system configuration of Fig. 3 is considered. It is obvious from Fig. 4 that optimized power allocation offers significant performance gains compared to equal power allocation, irrespective of the

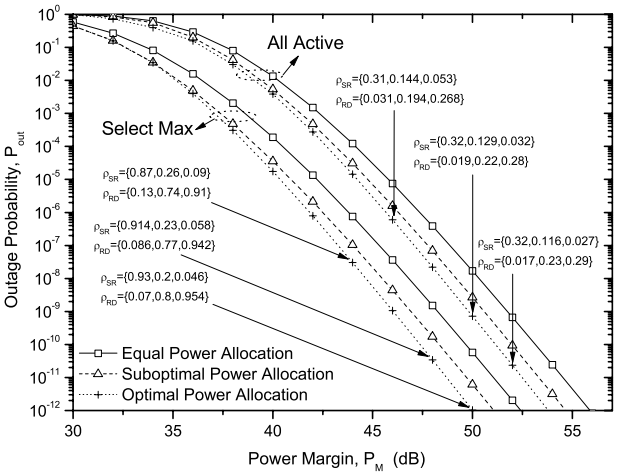

Fig. 4. Comparison of the power allocation schemes for the relaying protocols under consideration.

employed relaying protocol. This was expected, since both the path loss and turbulence strength are distance dependent in FSO links, and, hence, power allocation schemes that take into consideration the distances of the underlying links can significantly improve system performance. Furthermore, it is observed that even the simple suboptimal power allocation schemes lead to substantial performance improvements compared to equal power allocation. Taking into consideration that the parameters for the suboptimal schemes can be easily obtained, based only on system parameters that are known *a priori* at both the transmitter and the relays (since the link distances are fixed for most FSO applications), the proposed suboptimal power allocation can be considered as a less complex alternative to optimal power allocation.

VI. Conclusions

We investigated several transmission protocols for cooperative FSO systems for the Gamma–Gamma channel model. Alternative protocols to the all-active relaying scheme were proposed, which activate only a single relay in each transmission slot. This offers considerable benefits in terms of implementation complexity, since it avoids the need to synchronize the transmissions of multiple relays. In particular, two different types of relay selection protocol were proposed: select-max and DSS. Select-max relaying offers significant performance gains compared to the all-active scheme at the expense of requiring the CSI of all the available links. DSS relaying has identical performance to select-max relaying for $N = 2$, but it does not offer performance gains when $N > 2$, since it exploits only the two relays with the minimum max-equivalent distance; however, it can be considered as a less complex alternative to select-max, due to its limited CSI requirements. Furthermore, the problem of allocating the power resources to the FSO links was addressed, in order to account for the distance-dependent nature of atmospheric effects, and optimal and more computationally attractive suboptimal solutions were derived for each considered relaying protocol. Numerical results were provided, which clearly demonstrated the improvements in power efficiency offered by the proposed power allocation schemes.

APPENDIX A

Using the infinite series representation of the Gamma–Gamma pdf [25, Eqs. (7) and (8)], and since $\mathscr{P}_{o,AB} = \int_0^{\frac{1}{\bar{h}_{AB}\rho_{AB}P_M}} f_{\tilde{h}_{AB}}(x)dx$, after some basic algebraic manipulations the outage probability for the FSO link between terminals A and B can be obtained as

$$\mathscr{P}_{o,AB} = \frac{\pi}{\sin(\pi(\alpha_{AB}-\beta_{AB}))\Gamma(\alpha_{AB})\Gamma(\beta_{AB})} \sum_{l=0}^{\infty} \left(\frac{\frac{1}{(\beta_{AB}+l)}}{l!} \left(\frac{\frac{\alpha_{AB}\beta_{AB}}{P_M}}{\bar{h}_{AB}\rho_{AB}} \right)^{\beta_{AB}} \right.$$
$$\left. \times \left(\frac{\alpha_{AB}\beta_{AB}}{\bar{h}_{AB}\rho_{AB}} \right)^{l} - \frac{\frac{1}{(\alpha_{AB}+l)}}{l!} \left(\frac{\frac{\alpha_{AB}\beta_{AB}}{P_M}}{\bar{h}_{AB}\rho_{AB}} \right)^{\alpha_{AB}+l} \right). \quad (54)$$

For high values of the power margin, i.e., $P_M \to \infty$, the term for $l = 0$ is dominant and, hence, after using Euler's reflection formula [15, Eq. (8.334.3)] and introducing p_{AB} and q_{AB}, Eq. (54) can be approximated by Eq. (21). This concludes the proof.

APPENDIX B

Based on the infinite series representation of the Gamma–Gamma pdf [25, Eqs. (7) and (8)] and the Laplace transform, the MGF of $\xi_m = \rho_{R_mD} h_{R_mD}$ can be obtained as[4]

$$\mathscr{M}_{\xi_m}(s) = \frac{\left(\frac{\alpha_{R_mD}\beta_{R_mD}}{\bar{h}_{R_mD}\rho_{R_mD}} \right)^{q_{R_mD}} \Gamma\left(p_{R_mD} - q_{R_mD}\right)}{\Gamma(\alpha_{R_mD})\Gamma(\beta_{R_mD})} \times s^{-q_{R_mD}} + o\left(s^{-q_{R_mD}}\right). \quad (55)$$

Hence, the MGF for $h_{\mathscr{S}(n)} = \sum_{m\in\mathscr{S}(n)} \xi_m$ can be written as

$$\mathscr{M}_{h_{\mathscr{S}(n)}}(s) = \prod_{m\in\mathscr{S}(n)} \frac{\left(\frac{\alpha_{R_mD}\beta_{R_mD}}{\bar{h}_{R_mD}\rho_{R_mD}} \right)^{q_{R_mD}} \Gamma\left(p_{R_mD} - q_{R_mD}\right)}{\Gamma(\alpha_{R_mD})\Gamma(\beta_{R_mD})} \times s^{-\sum_{m\in\mathscr{S}(n)} q_{R_mD}} + o\left(\frac{1}{s^{\sum_{m\in\mathscr{S}(n)} q_{R_mD}}} \right), \quad (56)$$

and by taking the inverse Laplace transform of Eq. (56), an expression for the pdf of $h_{\mathscr{S}(n)}$ is obtained as

$$f_{h_{\mathscr{S}(n)}}(x) = \prod_{m\in\mathscr{S}(n)} \left(\frac{\alpha_{R_mD}\beta_{R_mD}}{\bar{h}_{R_mD}\rho_{R_mD}} \right)^{q_{R_mD}} x^{\left(\sum_{m\in\mathscr{S}(n)} q_{R_mD}\right)} \times \frac{\prod_{m\in\mathscr{S}(n)} \frac{\Gamma(q_{R_mD})\Gamma(p_{R_mD}-q_{R_mD})}{\Gamma(\alpha_{R_mD})\Gamma(\beta_{R_mD})}}{\Gamma\left(\sum_{m\in\mathscr{S}(n)} q_{R_mD}\right) x} + o\left(x^{\sum_{m\in\mathscr{S}(n)} q_{R_mD}+1}\right). \quad (57)$$

[4] We use the standard notation $f(x) = o(g(x))$, $g(x) > 0$ to state that $\frac{f(x)}{g(x)} \to 0$ as $x \to \infty$.

After some basic algebraic manipulations and keeping only the dominant term, the asymptotic expression in Eq. (25) is obtained for the cdf of $h_{\mathscr{S}(n)}$. This concludes the proof.

ACKNOWLEDGEMENT

Part of this paper was presented at the IEEE Global Communications Conference (GLOBECOM'11), December 2011.

REFERENCES

[1] H. Willebrand and B. S. Ghuman, *Free Space Optics: Enabling Optical Connectivity in Today's Networks*. Sams Publishing, 2002.

[2] L. Andrews and R. L. Philips, *Laser Beam Propagation Through Random Media*. SPIE Press, 2005.

[3] X. Zhu and J. M. Kahn, "Performance bounds for coded free-space optical communications through atmospheric turbulence channels," *IEEE Trans. Commun.*, vol. 51, pp. 1233–1239, Aug. 2003.

[4] M. L. B. Riediger, R. Schober, and L. Lampe, "Fast multiple-symbol detection for free-space optical communication," *IEEE Trans. Commun.*, vol. 57, pp. 1119–1128, Apr. 2009.

[5] X. Zhu and J. M. Kahn, "Free-space optical communication through atmospheric turbulence channels," *IEEE Trans. Commun.*, vol. 50, pp. 1293–1300, Aug. 2002.

[6] E. Lee and V. Chan, "Part 1: Optical communication over the clear turbulent atmospheric channel using diversity," *IEEE J. Sel. Areas Commun.*, vol. 22, pp. 1896–1906, Nov. 2004.

[7] S. G. Wilson, M. Brandt-Pearce, C. Qianling, and J. H. Leveque, "Free-space optical MIMO transmission with Q-ary PPM," *IEEE Trans. Commun.*, vol. 53, pp. 1402–1412, Aug. 2005.

[8] M. Safari and M. Uysal, "Relay-assisted free-space optical communication," *IEEE Trans. Wireless Commun.*, vol. 7, pp. 5441–5449, Dec. 2008.

[9] M. Kamiri and N. Nasiri-Kerari, "BER analysis of cooperative systems in free-space optical networks," *J. Lightwave Technol.*, vol. 27, pp. 5639–5647, Dec. 2009.

[10] M. Kamiri and N. Nasiri-Kerari, "Free-space optical communications via optical amplify-and-forward relaying," *J. Lightwave Technol.*, vol. 29, pp. 242–248, Jan. 2011.

[11] C. Abou-Rjeily and A. Slim, "Cooperative diversity for free-space optical communications: transceiver design and performance analysis," *IEEE Trans. Commun.*, vol. 53, pp. 658–663, Mar. 2011.

[12] C. Abou-Rjeily and S. Haddad, "Cooperative FSO systems: Performance analysis and optimal power allocation," *J. Lighwave Technol.*, vol. 29, pp. 1058–1065, Apr. 2011.

[13] H. S. Nalwa, *Handbook of Organic Electronics and Photonics*. American Scientific Publishers, 2006.

[14] M. Yano, F. Yamagishi, and T. Tsuda, "Optical MEMS for photonic switching–compact and stable optical crossconnect switches for simple, fast, and flexible wavelength applications in recent photonic networks," *IEEE J. Sel. Topics Quantum Electron.*, vol. 11, pp. 383–394, Mar. 2005.

[15] I. S. Gradshteyn and I. M. Ryzhik, *Table of Integrals, Series, and Products*, 7th ed. Academic, 2007.

[16] T. A. Tsiftsis, "Performance of heterodyne wireless optical communication systems over Gamma–Gamma atmospheric turbulence channels," *Electron. Lett.*, vol. 44, pp. 372–373, Feb. 2008.

[17] D. S. Michalopoulos and G. K. Karagiannidis, "Two-relay distributed switch and stay combining (DSSC)," *IEEE Trans. Commun.*, vol. 56, pp. 1790–1794, Nov. 2008.

[18] N. Letzepis, I. Holland, and W. G. Cowley, "The Gaussian free space optical MIMO channel with Q-ary pulse position modulation," *IEEE Trans. Wireless Commun.*, vol. 27, pp. 1744–1753, May 2008.

[19] M. K. Simon and M.-S. Alouini, *Digital Communication Over Fading Channels*, 2nd ed. John Wiley & Sons, New York, 2005.

[20] P. S. Bithas, N. C. Sagias, P. T. Mathiopoulos, G. K. Karagiannidis, and A. A. Rontogiannis, "On the performance analysis of digital communications over generalized-K fading channels," *IEEE Commun. Lett.*, vol. 10, pp. 353–355, May 2006.

[21] A. Papoulis and S. U. Pillai, *Probability, Random Variables and Stochastic Processes*, 4th ed. McGraw Hill, 2002.

[22] D. J. T. Heatley, D. R. Wisely, I. Neild, and P. Cochrane, "Optical wireless: The story so far," *IEEE Commun. Mag.*, vol. 36, pp. 72–74, Dec. 1998.

[23] J. Nocedal and S. J. Wright, *Numerical Optimization*. Springer, 1999.

[24] B. Anderson, J. Jackson, and M. Sitharam, "Descartes' rule of sign revisited," *Am. Math. Monthly*, vol. 105, pp. 447–451, May 1998.

[25] E. Bayaki, R. Schober, and R. Mallik, "Performance analysis of MIMO free-space optical systems in Gamma–Gamma fading," *IEEE Trans. Commun.*, vol. 57, pp. 1119–1128, Nov. 2009.